Agriculture, Ecosystems and Environment 146 (2012) 113–120

Contents lists available at SciVerse ScienceDirect

Agriculture, Ecosystems and Environment

journal homepage: www.elsevier.com/locate/agee

Estimation of Southeast Asian rice paddy areas with different ecosystems from moderate-resolution satellite imagery

Arika Bridhikitti[a,*], Thomas J. Overcamp[b]

[a] Faculty of Environment and Resource Studies, Mahasarakham University, Muang District, Maha Sarakham 44000, Thailand
[b] Department of Environmental Engineering and Earth Sciences, Clemson University, 342 Computer Court, L.G. Rich Environmental Lab, Anderson, SC 29625, USA

ARTICLE INFO

Article history:
Received 21 May 2011
Received in revised form 3 August 2011
Accepted 18 October 2011
Available online 22 November 2011

Keywords:
Moderate Resolution Imaging Spectroradiometer (MODIS)
Rice ecosystems
Southeast Asian rice paddy
Time-series satellite imagery

ABSTRACT

Multi-temporal satellite imagery from the Moderate Resolution Imaging Spectrometer (MODIS) was used to map the different ecosystems of Southeast Asian (SEA) rice paddies. The algorithm was based on temporal profiles of vegetation strength and/or water content, using MODIS surface reflectance in visible to near-IR range. The results obtained from the analysis were compared to national statistics. Estimated SEA regional rice area was 42×10^6 ha, which agrees with published values. The model performance was dependent on rice ecosystems. Good linear relationships between the model results and the national statistics were observed for rainfed rice. High linear coefficients of determination, R^2, were also found for irrigated rice and upland rice, but the model tended to underestimate irrigated rice and overestimate upland rice. However, these high R^2 values indicated that the model effectively simulated spatial distribution of these rice areas. These R^2 values were either of similar magnitude or larger than those reported in literature, regardless of the rice ecosystem. Poor correlation was observed for deepwater rice.

1. Introduction

Southeast Asian (SEA) rice paddy areas are approximately 30% of the world total (Huke and Huke, 1997; Hays et al., 2005). Rice is a food crop and export commodity in the region. Spatial information of SEA rice paddies is required for regional rice cropping/water managements and estimates of rice yield. Necessary information for informed management includes rice cropping frequency, rice ecosystem type (irrigated, rainfed lowland, upland, and flood-prone), and areal distribution. This research applies the multi-temporal satellite imagery for mapping rice paddies with different rice ecosystems over SEA.

In addition, previous global-scale methane measurements taken from NASA's Earth Observing System satellites have shown that methane emissions due to both biomass burning and rice cultivation from SEA are significant (Xiong et al., 2008; Payne et al., 2009). The magnitudes of methane emissions strongly depend on type of rice ecosystem (Chareonsilp et al., 2000; Wassmann et al., 2000; Yan et al., 2003; Hays et al., 2005).

The Moderate Resolution Imaging Spectrometer (MODIS) is an instrument onboard the Terra and Aqua satellites. The first MODIS flight instrument was launched in December 1999 (Justice et al., 2002). In contrast to data from higher resolution satellites (such as Landsat, SPOT VGT), MODIS data have daily observations, which are more useful for studies concerning vegetation phenology (Huete et al., 2008; Tingting and Chuang, 2010). In addition, analyzing higher resolution satellite data requires higher-level computational resources and has higher costs associated with data acquisition and processing (Tingting and Chuang, 2010). Land analyses using time-series MODIS retrievals have been widely conducted for detecting vegetation and its changes (Xiao et al., 2005, 2006; Hayes and Cohen, 2007; Huete et al., 2008; Wardlow and Egbert, 2008; Sakamoto et al., 2009; Sun et al., 2009; Tingting and Chuang, 2010; Chen et al., 2011; Peng et al., 2011).

Xiao et al. (2005, 2006) introduced algorithms for estimating rice paddy areas for Southern China, and South and Southeast Asia, respectively, using multi-temporal MODIS imagery analysis. These analyses were based on the temporal correspondence between the water index and vegetation indices. Their results show the linear coefficient of determination (R^2) between the MODIS-estimated rice areas and provincial-scale national statistics ranging from 0.42 to 0.87 for SEA countries. Sun et al. (2009) modified this algorithm to obtain spatial distribution of paddy rice with different growth calendar regionalization (including single, early, and late rice) for China. Because of problems associated with cloud contamination and coarse spatial resolution of the MODIS data, their results showed this technique was unsuitable for monitoring the interannual variations of the rice planted area. Peng et al. (2011) also improved this technique by gap-filling cloud contaminated pixels with an interpolation filter. Their work was focused at the county

* Corresponding author. Tel.: +66 43754333x6622; fax: +66 43742135.
E-mail address: arika.b@msu.ac.th (A. Bridhikitti).

0167-8809/$ – see front matter © 2011 Elsevier B.V. All rights reserved.
doi:10.1016/j.agee.2011.10.016

scale for Hunan Province, China. Their results had R^2 values of 0.58, 0.52, and 0.34 for single, early, and late rice, respectively.

This is the first study extending the work of Xiao et al. (2005, 2006) for mapping SEA rice paddies with different rice ecosystems. The modified algorithm developed in this study was based solely on observed SEA rice phenology. It is a simple method that can be applied at the regional scale. In addition, the results also include spatial information on rice cropping frequency. This information can be further used to quantitatively estimate air pollution emissions from SEA rice paddies and evaluate climate change effects attributed to the emissions.

2. Methodology

2.1. Description of study area

SEA can be divided into two geographic regions: the mainland and the islands. The mainland consists of the countries of Cambodia, Lao PDR, Myanmar, Thailand, and Vietnam. The larger islands are the countries of Brunei, East Timor, Indonesia, Malaysia, Philippines, and Singapore. The latitude of this region ranges from 7°S to 20°N, and its longitude is from 95° to 130°E.

The climate of SEA is tropical, hot and humid year round. NE winds bring in drier, cooler air from mainland China causing a dry season from November to mid-March for most of SEA mainland. These NE winds bring severe weather to the SEA islands. The milder SW prevailing winds are from mid-May to September. These winds bring wet air masses from the Indian Ocean causing a wet season over the entire region.

2.2. Data description

2.2.1. MODIS imagery data

The MODIS surface reflectance 8-day L3 Global 500 m SIN Grid V005, or MOD09A1, data set from 2006 to 2007 was acquired for this study. Each grid value gives the percentage of the radiant energy in the specific bandwidth to the total energy integrated over the entire spectrum. In this study, the MODIS surface reflectance in four spectral bands, in the visible and near-infrared, was considered. These are band 1: 620–670 nm (visible-red: VISR), band 2: 841–876 nm (near-infrared: NIR), band 3: 459–479 nm (visible-blue: VISB), and band 6: 1628–1652 nm (shortwave-infrared: SWIR). The products were downloaded from the USGS Land Processes Distributed Active Archive Center (LPDAAC, 2008). The MODIS surface reflectance data used in this study were restricted to those with a Science Quality Flag of "Passed" or "Inferred Passed." This Science Quality Flag is metadata summarizing the results of quality assessment procedures performed by the NASA scientist team after the products are generated (Roy et al., 2002). In addition, zero percent cloud coverage was flagged for all observations in this data set.

These reflectance products are reported at a 500-m resolution in a level 3, grid projection. Each pixel contains the best possible L2G (daily) observation during an 8-day period. These version 5 reflectance products are validated stage 1, meaning that accuracy has been estimated using a small number of independent measurements obtained from selected locations and time periods and ground-truth/field program efforts (LPDAAC, 2008). The products are in HDF-EOS format. Prior to the analysis, these data were converted to GeoTIFF format and reprojected to UTM zone 48 projected coordinate system with the WGS1984 (the World Geodetic Survey System of 1984) datum by using MODIS Reprojection Tool (MRT) from USGS/LPDAAC (LPDAAC, 2008). These reprojected data sets were used in the land classification analyses running on the Modelbuilder in ArcGIS 9.2 software with integrated Python scripts.

2.2.2. Ancillary data

2.2.2.1. Global 30 arc-second elevation data set, GTOPO30. The GTOPO30 data set was acquired from the US Geological Survey (USGS) website (http://edc.usgs.gov/products/elevation/gtopo30.html). This is a global raster digital elevation model (DEM) with a horizontal grid spacing of 30 arc seconds (approximately 1 km). These data are expressed in geographic coordinates and referenced to WGS1984 datum. This DEM was used to generate a mask of the elevation above 2500 m or regions having a slope greater than 30°. Since rice is not usually grown at higher elevations or steeper slopes (IRRI, 1975), these areas were excluded from the rice paddy map.

2.2.2.2. SEA administrative boundary coverage map. The country administrative base maps were downloaded from the International Potato Center data server (CIP, 2008). These maps are polygon shapefiles expressed in geographic coordinates and referenced to WGS1984. The maps provide the administrative boundary coverage at the provincial/state level.

2.3. Data processing

2.3.1. Surface reflectance enhancement

The normalized difference vegetation index (NDVI), the enhanced vegetation index (EVI), the normalized build-up index (NDBI), and the land surface water index (LSWI: negative NDBI) are calculated from the surface reflectance, ρ, in visible-red (VISR; MODIS-band 1), near-infrared (NIR; MODIS-band 2), visible-blue (VISB; MODIS-band 3), and shortwave-infrared (SWIR; MODIS-band 6) using the following equations (Zha et al., 2003; Xiao et al., 2005, 2006).

$$\mathrm{NDVI} = \frac{\rho_{\mathrm{NIR}} - \rho_{\mathrm{VISR}}}{\rho_{\mathrm{NIR}} - \rho_{\mathrm{VISR}}} \quad (1)$$

$$\mathrm{EVI} = 2.5 \times \frac{\rho_{\mathrm{NIR}} - \rho_{\mathrm{VISR}}}{\rho_{\mathrm{NIR}} + 6\rho_{\mathrm{VISR}} - 7.5\rho_{\mathrm{VISB}} + 1} \quad (2)$$

$$\mathrm{NDBI} = \frac{\rho_{\mathrm{SWIR}} - \rho_{\mathrm{NIR}}}{\rho_{\mathrm{SWIR}} - \rho_{\mathrm{NIR}}} \quad (3)$$

NDVI and EVI were used in this study to enhance the vegetation detection sensitivity of the MODIS surface reflectance. Both indices are estimated by normalizing the difference between the radiances in the near-infrared spectra and in the red-visible spectra. In addition, EVI incorporates the additional blue band to correct for aerosol influences in the red band and the canopy background adjustment (Huete et al., 2002). In this study, the time-series NDVIs were used to identify forests, which include perennial and seasonal plantations. The time-series EVIs were used to identify rice paddies with different ecosystems because of its higher sensitivity to canopy structural variation (Huete et al., 2002; Motohka et al., 2009).

Zha et al. (2003) introduced NDBI to automate the process of mapping built-up areas. NDBI is the negative of LSWI. Both indices are calculated from the normalized difference between the radiance in shortwave-infrared spectra and in near-infrared spectra.

The time-series NDVI, EVI, and NDBI or LSWI raster maps were imported to the rice paddy analysis model to create flooding and transplanting (FT) binary maps from the math algebra of either $\mathrm{LSWI} + 0.05 \geq \mathrm{EVI}$ (Xiao et al., 2005, 2006) or $\mathrm{LSWI} \geq 0.18$.

2.3.2. Forest mask

Bridhikitti (2011) observed temporal distribution of NDVI over selected forest and plantation areas in SEA. From those observations, evergreen forests and perennial plantations (mainly rubber, oil palm, and coconut plantations) were consistently observed having $\mathrm{NDVI} > 0.7$. Deciduous forests and seasonal plantations exhibited lower mean NDVIs with higher annual variation from

0.55 to 0.75 due to interference by high annual soil moisture variations. Mangrove forests, with wetland backgrounds, exhibited high NDVI variation ranging from <0.1 to >0.8 (Bridhikitti, 2011).

Corresponding to the observations, evergreen forests and perennial plantations were identified as any pixel having NDVI ≥ 0.7 for at least half of the 46 consecutive 8-day maps. Deciduous forests and seasonal plantations were identified as any pixel having NDVI ≥ 0.7 for at least one third of the observations and flooding and transplanting, FT, was observed for less than half of the observations. Wetland and mangrove forests were identified as any pixel having NDVI ≥ 0.7 for at least one third and FT for at least half of the observations.

2.3.3. Urban mask

Bridhikitti (2011) showed that built-up surfaces can be identified from any pixel having 0.1 < NDVI < 0.5 and NDBI > −0.15 for at least half of the 46 consecutive maps. By using these criteria, built-up surfaces as well as highly light-reflecting soils were determined (Bridhikitti, 2011). These highly reflecting soils are found in the central dry zone in Myanmar and in northeastern Thailand. These soils are used for growing rainfed rice, wheat, and other short-growing-season crops. Bridhikitti (2011) suggested that annual NDBI variance, calculated using Eq. (4), can be used to differentiate built-up surfaces from these soils. High NDBI variance was found for the soils due to soil–vegetation transition, and lesser variation was found over the built-up surfaces (Bridhikitti, 2011).

$$\text{NDBI variance} = \frac{\sum_1^{46} \text{NDBI}^2 - 46 \times \left(\overline{\text{NDBI}}\right)^2}{46} \quad (4)$$

Based on the results in the work of Bridhikitti (2011), areas with lower NDBI variance (<0.0086) were assigned to built-up surfaces. In the case of low- to medium-intensity developed areas or urban areas having large green areas, this analysis tends to have high omission error (Bridhikitti, 2011), but this was minimized by merging the results from two consecutive years (2006 and 2007 for this study).

2.3.4. Mapping SEA rice paddies

In this study, different rice ecosystems and the annual cropping frequency are identified from rice canopy development patterns. The four major rice ecosystems as categorized by International Rice Research Institute (IRRI) are: irrigated, rainfed lowland, upland, and flood-prone. All four ecosystems can be found in SEA. Their characteristics are detailed in the following:

Irrigated rice is grown in fields with assured irrigation for one or more crops a year. It is planted in leveled, diked fields with water control. Rice can either be transplanted from nursery mats or directly seeded in puddled soil. Intermediate fallow periods range from a few days to three months.

Rainfed lowland rice is grown only once a year during the wet season when there is sufficient water from rain. It is planted in leveled to slightly sloping, diked fields with non-continuous flooding. The water level does not exceed 50 cm for more than ten consecutive days. Rice can either be transplanted in puddled soil or directly seeded on puddled or plowed dry soil.

Deepwater rice or *flood-prone rice* has only one crop per year during the wet season when natural flooding occurs. It is planted in leveled to slightly sloping or depressed fields. Water levels range from 50 to more than 300 cm for more than 10 consecutive days in growth stage. Rice can either be transplanted in puddled soil or directly seeded on plowed dry soil.

Upland rice can grow in both flat and sloping fields, which rarely flood and are not diked. This rice is prepared and directly seeded on plowed dry soil or dibbled in wet soil that depends on rainfall for moisture (IRRI, 1975).

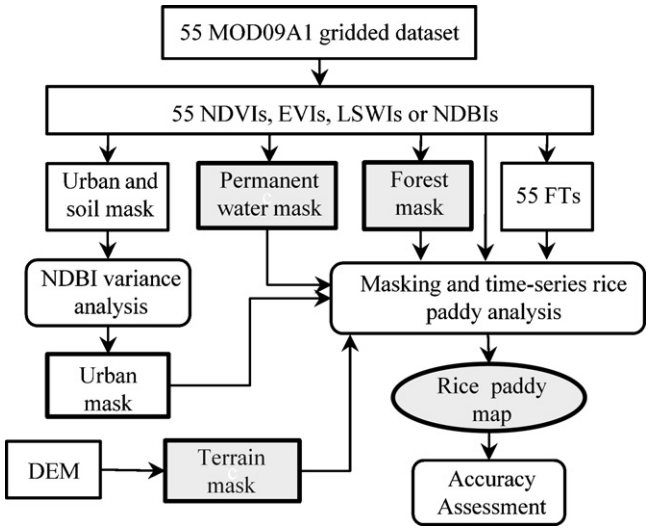

Fig. 1. Schematic diagram showing the methodology used for mapping rice paddy in this study. *Note:* NDVI = normalized difference vegetation index; EVI = enhanced vegetation index; LSWI = land surface water index; NDBI = normalized build-up index; FT = flooding and transplanting binary; DEM = digital elevation model.

A rice-cropping cycle takes three to six months depending on the rice ecosystems. Rice canopy development is generally divided into three phases:

(1) Vegetative phase occurs around 60 days after sowing. Generally, germination and early seeding stages are prepared in nursery mats and then transplanted into puddled, leveled fields. The water signature dominates during transplanting.
(2) Productive phase starts around 60 days after sowing or 30 days after transplanting and lasts until the 90th day. Plants rapidly grow and reach fully developed height. The plant canopies cover most of the water surface, intensifying the vegetation signature.
(3) Ripening phase is from 90th day to about 120th day. Golden grains start developing. The vegetation signature is still dominant but lessens due to drying leaves. This period could be extended to six months in the case of deepwater rice.

The algorithm for mapping rice paddies uses time-series MODIS retrievals to identify SEA rice paddies with different ecosystems. This algorithm is a modification of research conducted by Xiao et al. (2005, 2006) estimating rice paddy areas for Southern China, and South and Southeast Asia, respectively, using multi-temporal MODIS images analysis. However, Xiao et al. (2005, 2006) do not identify different rice ecosystems. The major modifications of the work of Xiao et al. (2005, 2006) in this study are: (1) different constraints for terrain mask that allows for steeper slopes and higher altitudes, (2) temporal patterns and strengths of the vegetation–water signals that are more adaptive to specific vegetation-canopy developments in different rice ecosystems, and (3) the inclusion of deciduous forests/seasonal plantations and urban masks.

The schematic diagram used for mapping the rice paddy areas in this study is shown in Fig. 1. The 55 data sets of the 8-day composite (440 days) surface reflectance band 1, 2, 3, and 6 were used to create 55 consecutive NDVI, EVI, LSWI or NDBI, and FT raster maps. These series maps were then used to create the non-rice paddy area masks, which include forest, built-up area, permanent water, and terrain. The algorithms for creating forest and built-up area masks were given in Sections 2.3.2 and 2.3.3, respectively. The algorithms for permanent water and terrain are detailed below.

- The permanent water mask consists of pixels having NDVI < 0.1 and LSWI > 0 for at least one-third of the 46 consecutive maps (368 days). This algorithm provides sufficient sensitivity for identifying the major water resources, such as Mekong River, Irrawaddy River in Myanmar, Red River in Vietnam, Tonlé Sap Lake in Cambodia, Songkhla Lake in Thailand, Inle Lake in Myanmar, and Laguna de Bay in the Philippines.
- Upland rice can be found on slopes up to 30° (Ahmadi et al., 2004) and elevations up to 2500 m (IRRI, 1975). For upland rice in this study, the terrain mask is restricted to areas having elevation greater than 2500 m or slopes greater than 30°. Since Xiao et al. (2005, 2006) defined the terrain mask as elevations greater than 2000 m or slopes greater than 2°, this work expands potential areas of rice cultivation.

A total of 55 EVI consecutive maps (440 days) were used for a complete one-year analysis. After masking, time-series analysis was performed using the following algorithms in order.

- The deepwater rice candidates are assumed to be the pixels having FT for more than 38 of the total 55 consecutive maps, slopes ≤2°, and elevations <600 m. The true deepwater rice pixels are those candidates that have EVI higher than half of the maximum EVI in the next five 8-day (40 days) composites following the date observing FT. The EVI must continue rising to higher than 0.6 of EVI maximum in the next nine 8-day composites.
- The rainfed rice candidates are assumed to be the pixels having FT for 4–20 maps of the total, and slope ≤2°. The true rainfed rice pixels are the candidates that have both EVI higher than half of the maximum EVI in the next six 8-day composites following the date observing FT and the EVI must continue rising higher than 0.7 of the EVI maximum in the next eight 8-day composites.
- The irrigated rice candidates are assumed to be the pixels having FT for 16–38 maps of the total and slopes ≤2°. The true irrigated rice pixels are the candidates that have EVI higher than half of the maximum EVI in the next five 8-day composites following the date observing FT. This EVI continues rising to higher 0.6 than the EVI maximum in the next six composites.
- The true upland rice pixels are identified using the same algorithms as the ones for rainfed rice and irrigated rice but with slopes >2°.

Table 1
The sources of the national statistical databases used in this study for accuracy assessment.

Country	National rice paddy area database
Indonesia	2007 National rice paddy areas acquired from Badan Pusat Statistik (BPS, 2008)
Lao PDR	2006 Rice paddy areas acquired from the National Statistics Center of the Lao PDR (NSC, 2008)
Philippines	2006 Rice paddy areas acquired from the National Statistics Office of Philippines (NSOP, 2008)
Thailand	2003 National rice paddy areas acquired from the National Statistical Office of Thailand (NSOT, 2008)
Vietnam	2006 Rice paddy areas acquired from the General Statistics Office of Vietnam (GSO, 2008)

2.4. Accuracy assessment

The national statistics of forest, perennial plantation, and rice paddy areas were acquired from the sources listed in Table 1 to compare with the results obtained from the MODIS time-series models. These comparisons were done on a provincial/state level.

3. Results and discussion

3.1. Spatial distribution of SEA rice paddy areas with different ecosystems and cropping frequencies

Fig. 2 shows the spatial distributions of the predicted rice ecosystem over SEA. As seen from this map, the rainfed rice ecosystem dominated over NE Thailand, central Myanmar, and Cambodia.

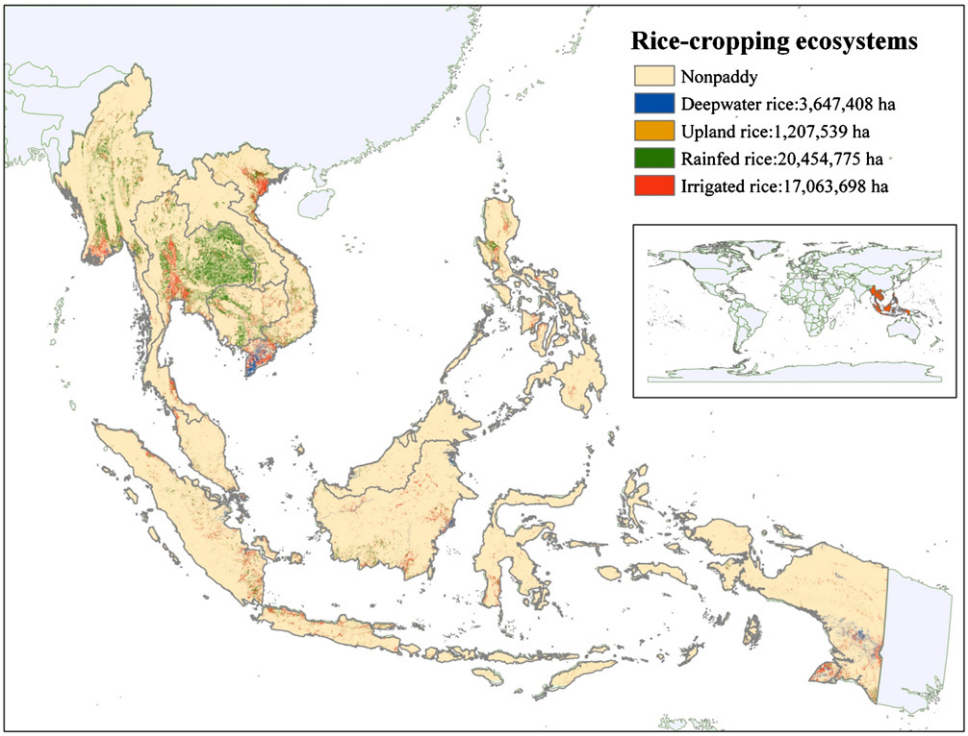

Fig. 2. Spatial rice paddy distribution map over SEA by rice ecosystem generated from time-series MODIS imagery analysis.

Table 2
The percentage of area by rice ecosystem, and by rice cropping frequency, and the total rice paddy areas acquired from FAOSTAT Database and estimated from the MODIS-derived model by country.

Country	MODIS-derived model (2006 and 2007)								Total areas mid-1990s[a], 10^3 ha	FAO total areas 2005[b],10^3 ha
	Rice ecosystem, %				Cropping frequency, %			Total areas, 10^3 Ha		
	Deepwater	Upland	Rainfed	Irrigated	Single	Double	Multi			
Myanmar	0.97	6.40	61.71	30.91	78.51	19.12	2.37	6157	6285	6270
Vietnam	15.58	6.86	28.75	48.81	78.86	17.91	3.23	5762	6375	7340
Cambodia	4.71	3.41	60.96	30.93	72.26	22.35	5.40	1961	1899	2150
Lao PDR	0.00	4.73	75.38	19.89	83.49	15.02	1.48	1129	611	736
Thailand	0.97	1.43	75.07	22.54	81.39	16.44	2.18	11,994	9644	10,200
Philippines	1.32	0.52	70.10	28.06	76.60	20.27	3.13	2827	3620	4000
Malaysia	13.99	0.83	26.04	59.14	68.27	23.66	8.06	994	668	660
Indonesia	19.99	0.90	19.79	59.31	67.92	22.20	9.88	11,511	11,015	11,801
Brunei	17.31	0.38	28.86	53.45	74.03	21.20	4.77	17	–	–
Singapore	4.20	0.00	65.52	30.28	58.62	30.93	10.45	20	–	–
Total								42,373	40,117	43,157

[a] Huke and Huke (1997).
[b] FAOSTAT (2006).

The irrigated rice ecosystem dominated central Thailand; Red River Delta, Vietnam; Irrawaddy River Delta, Myanmar; Central Luzon, Philippines; Songkhla Lake, Thailand; and Mekong River drainages in both Cambodia and Vietnam. The deepwater rice ecosystem was primarily observed in the Mekong River Delta, Vietnam; and in Papua, Indonesia. The single rice crops were approximately 32×10^6 ha for SEA. Approximately 10×10^6 ha was double- and multiple-rice crops, which were found in the major irrigated rice ecosystems.

The result from the model showed that the rice paddy area accounted for 8.7% of total SEA land area. The estimated total regional rice paddy area is 42.4×10^6 ha, which is consistent with

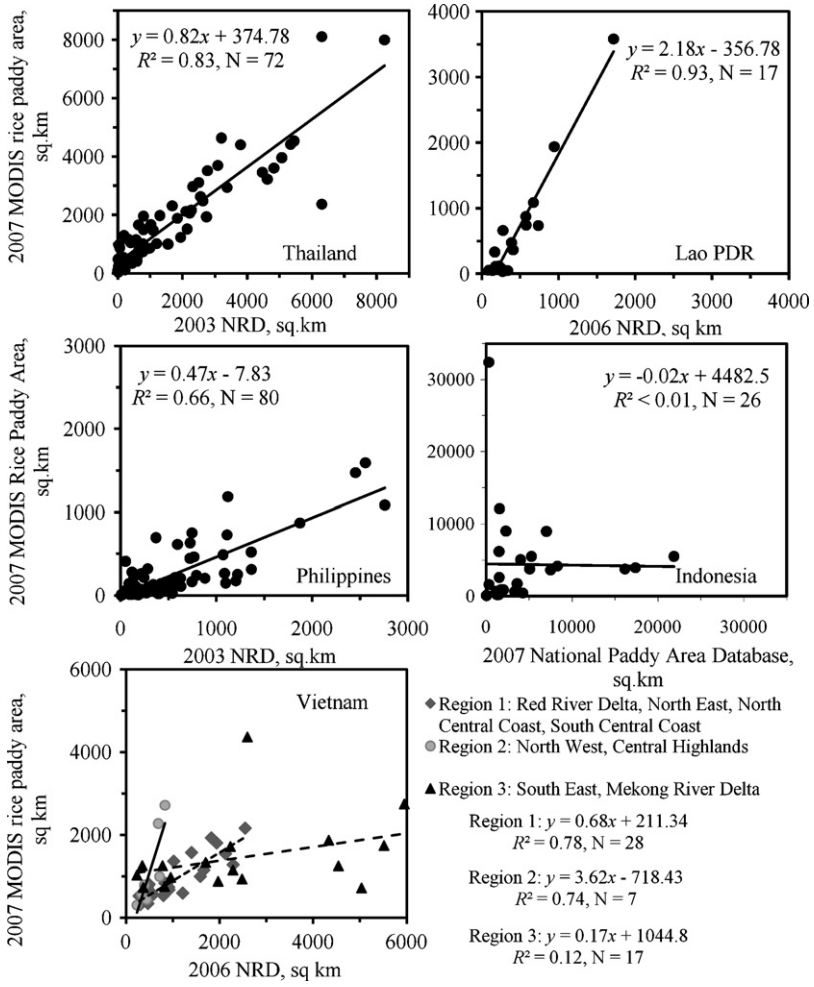

Fig. 3. Linear regression plots of the MODIS rice paddy areas and the rice paddy areas acquired from the national rice database by province (or state) for Indonesia, Philippines, Thailand, Lao PDR, and Vietnam.

the areas reported in FAOSTAT (2006), 42.2×10^6 ha, and by Huke and Huke (1997), 40.1×10^6 ha (see Table 2). Considering paddy areas by country, good agreement between the estimated and published values were found for Myanmar, Cambodia, Thailand, and Indonesia. The result for Cambodian rice area is improved compared to the estimate of Xiao et al. (2006), which was substantially higher than that reported in national statistical database. The estimates for Vietnam and the Philippines were low. Rice paddy area was overestimated for Lao PDR and Malaysia.

3.2. Comparisons between the modeled rice areas and the national statistics

The rainfed rice ecosystem dominated in Myanmar (62%), Cambodia (61%), Lao PDR (75%), Thailand (75%), and the Philippines (70%), as indicated from Table 2. The values obtained from this model for Myanmar and the Philippines were significantly higher than those reported by Huke and Huke (1997) by 40% and 35%, respectively. This might be a result of misclassifying multiple-irrigated rice as single-rainfed rice, as discussed below.

Fig. 3 shows the plots between the MODIS-estimated paddy areas (y) and the national rice paddy area statistics by province (x) for Indonesia, Philippines, Thailand, Lao PDR, and Vietnam. These plots suggest good correlations for Thailand with R^2 of 0.83 and for Lao PDR with R^2 of 0.93. The estimated rainfed rice ecosystem is approximately 75% of the total rice paddy area in both countries. Under this ecosystem, the temporal EVI and the water logic profiles, as seen in Fig. 4 for northeastern Thailand and Phnom Penh, Cambodia, clearly illustrate single rice canopy development (single annual cycle of EVI after the presence of water logic of unity), which can be easily predicted by the model.

The national rice statistics of Lao PDR reported that 13.6% of the total rice paddy area was upland rice (NSC, 2008). The ratio is higher than that estimated by the model, which was only 4.7% of the total. High uncertainty on the upland rice area estimation using a MODIS-derived model was also found in previous studies (Xiao et al., 2005, 2006). As seen in Fig. 3, the results over the major upland rice provinces in Lao PDR, and in the North West and the Central Highlands regions in Vietnam show that the MODIS rice areas are 2.2 times and 3.6 times, respectively, larger than those reported in the national statistics. Not only upland rice areas are overestimated in this study, but the general upland crops area was overestimated by. Tingting and Chuang (2010), who used MODIS NDVI to separate crop and non-crop areas in the Chao Phraya Basin, Thailand. They attributed this discrepancy to the similarity of the NDVI signals for the crops and adjacent grass or deciduous shrubs.

As indicated from the model's results in Table 2, irrigated rice paddies were predominant in Vietnam (49%), Malaysia (59%), and Indonesia (59%). Except for the Philippines, the irrigated rice areas were in similar magnitude to those reported by Huke and Huke (1997), which showed the prevalence of irrigated rice. The EVI and the water logic profiles in Fig. 4 over the selected irrigated rice paddy pixels in Hanoi, Vietnam clearly indicated double-rice crops. However, the profiles observed in South Kalimantan, Indonesia and Bataan, Philippines did not clearly show double-rice crops. In an irrigated ecosystem, there are sufficient water resources for multiple-rice cropping and each holder of rice paddies can have different rice cropping calendar. This causes inconsistent temporal patterns of the rice canopy development over large spatial scale. For this reason, the model tends to not include irrigated rice areas or misclassifies this rice as single rice in a rainfed ecosystem. Over the provinces dominated by irrigated rice cultivation in region 1 Vietnam, which consists of the Red River Delta, North East, North Central Coast, and South Central Coast, and in the Philippines (see Fig. 3), the MODIS rice areas were 0.68 and 0.47 times, respectively,

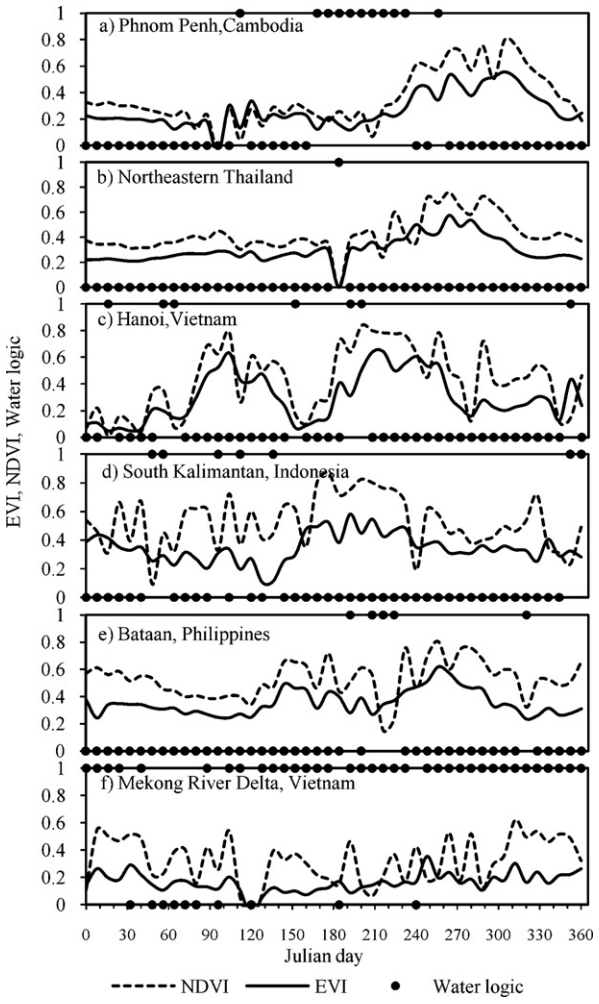

Fig. 4. Temporal EVI, NDVI, and water logic profiles at the selected rice paddy pixels.

smaller than those reported in the national databases with R^2 of 0.78 and 0.66, respectively.

The overall high R^2 values ($\geq$0.66) for the areas dominated by both total rice and rainfed rice, in the cases of Thailand, Lao PDR, Vietnam, and Philippines, indicate that the spatial distribution of these MODIS-derived rice paddy areas is consistent with actual distributions from the national statistics. Moreover, these R^2 values either have similar magnitudes or are larger than those reported by Xiao et al. (2006) for Thailand, Lao PDR, Vietnam, and Philippines, regardless of the rice ecosystem.

In the case of Indonesia, there was poor correlation between the estimated rice areas and the national rice statistics. One of the outlier estimates was observed in the Papua region. The model reports 3×10^6 ha rice paddies over this region, while the national rice statistics are only 0.02×10^6 ha. The cause of this discrepancy is not understood. This model predicts that deepwater and irrigated rice are dominant in southern Papua. In actuality, the major crops are root and tuber crops, such as yam, taro, sweet potato, vegetables, and fruits (Dixon et al., 2001). The poor correlations for the deepwater ecosystem were also observed in the South East and Mekong River Delta regions in Vietnam from the coefficient of determination shown in Fig. 3.

From Fig. 4, temporal EVI and the water logic profiles observed over a deepwater rice paddy grid in Mekong River Delta in Vietnam exhibited results similar to those of long-term wetlands. Thus this rice ecosystem could easily be misclassified as natural wetlands and

vice versa. The Mekong River Delta in Vietnam has heterogeneous agriculture consisting of deepwater rice paddies, irrigated rice paddies, and aquaculture farms (Pingali and Xuan, 1992; Sakamoto et al., 2009). MODIS data have coarse spatial resolution which could cause its poor ability to distinguish among these land uses.

There have been attempts to reduce the noise component in the time-series MODIS data collected over this region. Several mathematical techniques have been proposed which include wavelet-based filter (Sakamoto et al., 2005) and empirical mode decomposition (Chen et al., 2011). The techniques provide good results, which suggest that they are capable of resolving heterogeneity in mixed rice ecosystems (Sakamoto et al., 2009; Chen et al., 2011). However, efficiency and accuracy of using these noise reduction techniques in regional scale land analysis has not yet been proven.

4. Conclusions

In this study, Southeast Asian (SEA) rice paddies with different rice ecosystems were mapped using time-series satellite imagery analysis. This imagery was generated from the 500-m resolution MODIS/terra spectral surface reflectance (MOD09A1) data acquired from 2006 to 2007. The algorithm for mapping rice paddy area was developed based on the observed temporal SEA rice canopy developments. This algorithm distinguishes different rice ecosystems and provides rice-cropping frequency.

The total estimated rice area for SEA was 42×10^6 ha, which is consistent with published values. Comparison of the estimated rice paddy area (y) and the national rice statistics (x) on the provincial or state level show high linear correlations over the areas dominated by rainfed rice (i.e. Thailand: $R^2 = 0.83$, slope = 0.82 and Lao PDR: $R^2 = 0.93$, slope = 2.2). The high correlations were also found in irrigated rice, but the model tended to under estimate the paddy areas (i.e. Red River Delta in Vietnam: $R^2 = 0.78$, slope = 0.68, and Philippines: $R^2 = 0.66$, slope = 0.47). This could have resulted from the inconsistency of the temporal rice canopy development pattern over large-scale areas. For the areas dominated by upland rice, the correlations were good but the MODIS rice areas were overestimated (i.e. Lao PDR, and the highland regions in Vietnam: $R^2 = 0.74$, slope = 3.6). Overall high R^2 values indicate that spatial distribution of these MODIS rice areas was consistent with the actual distribution. In addition, these R^2 values either have similar magnitudes or are larger than those reported in literature, for all rice ecosystems. A poor correlation was observed for deepwater rice (i.e. Mekong River Delta in Vietnam: $R^2 = 0.12$) because this rice ecosystem could easily be misclassified as wetlands and vice versa and because of landuse heterogeneity.

This model can be used to identify SEA areas that are influenced by activities attributed to rainfed, irrigated, and upland rice culitvation. Model users could be state officers or inter-country partners working on regional water management for agriculture and on agricultural yield estimation. Atmospheric scientists can also employ the model's results to estimate regional budget and spatial loading of pollutants attributed to biomass burning and rice cultivation.

Acknowledgements

The author would like to thank the Royal Thai Government for granting a Ph.D. scholarship. The Clemson University Research Foundation supported the publication of these results.

References

Ahmadi, N., Dzido, J.L., Vales, M., Rakotoarisoa, J., Chabanne, A., 2004. Upland rice for highlands: new varieties and sustainable cropping systems for food security Promising prospects for the global challenges of rice production? In: Proceedings of the FAO Rice Conference, Rome, Italy, 12–13 February.

Badan Pusat Statistik (BPS), 2008. Statistics Indonesia Web Page: http://dds.bps.go.id/eng/ (accessed July 2008).

Bridhikitti, A., 2011. Applications of Moderate-Resolution Remote Sensing Technologies for Surface Air Pollution Monitoring in Southeast Asia, Ph.D. Dissertation, Clemson University, USA, 254 pp.

Chareonsilp, N., Buddhaboon, C., Promnart, P., Wassmann, R., Lantin, R.S., 2000. Methane emission from deepwater rice fields in Thailand. Nutr. Cycl. Agroecosys. 58, 121–130.

Chen, C., Son, N., Chang, L., Chen, C., 2011. Monitoring of soil moisture variability in relation to rice cropping systems in the Vietnamese Mekong Delta using MODIS data. Appl. Geogr. 31, 463–475.

CIP, Centro internacional de la papa: GIS data. Available Online at: http://research.cip.cgiar.org/gis/modules.php?name=Downloads&d_op=viewdownload&id=1 (accessed January 2008).

Dixon, J., Gulliver, A., Gibbon, D., 2001. Farming systems and poverty: improving farmers' livelihoods in a changing world. In: Hall, M. (Ed.), FAO and World Bank, Rome and Washington, DC.

FAOSTAT, 2006. Statistical Database of the Food and Agricultural Organization of the United Nations. Available Online at: http://faostat.fao.org/site/377/default.aspx#ancor (accessed December 2008).

GSO, General Statistics Office of Vietnam Web Page: http://www.gso.gov.vn/default_en.aspx?tabid=491 (accessed July 2008).

Hayes, D.J., Cohen, W.B., 2007. Spatial, spectral and temporal patterns of tropical forest cover change as observed with multiple scales of optical satellite data. Remote Sens. Environ. 106, 1–16.

Hays, M.D., Fine, P.M., Geron, C.D., Kleeman, M.J., Gullett, B.K., 2005. Open burning of agricultural biomass: physical and chemical properties of particle-phase emissions. Atmos. Environ. 39, 6747–6764.

Huete, A., Didan, K., Miura, T., Rodriguez, E.P., Gao, X., Ferreira, L.G., 2002. Overview of the radiometric and biophysical performance of the MODIS vegetation indices. Remote Sens. Environ. 83, 195–213.

Huete, A., Restrepo-Coupe, N., Ratana, P., Didan, K., Saleska, S.R., Ichii, K., Panuthai, S., Gamo, M., 2008. Multiple site tower flux and remote sensing comparisons of tropical forest dynamics in Monsoon Asia. Agric. Forest Meteorol. 148, 748–760.

Huke, R.E., Huke, E.H., 1997. Rice Area by Type of Culture: South, Southeast and East Asia. International Rice Research Institute, Los Banos, Philippines.

IRRI, 1975. Major Research in Upland Rice. International Rice Research Institute, Los Banos, Philippines.

Justice, C.O., Townshend, J.R.G., Vermote, E.F., Masuoka, E., Wolfe, R.E., Saleous, N., Roy, D.P., Morisette, J.T., 2002. A overview of MODIS Land data processing and product status. Remote Sens. Environ. 83, 3–15.

LPDAAC, 2008. Land Processes Distributed Active Archive Center Web Page: http://lpdaac.usgs.gov/datapool/datapool.asp (accessed March 2008).

Motohka, T., Nasahara, K.N., Miyata, A., Mano, M., Tsuchida, S., 2009. Evaluation of optical satellite remote sensing for rice paddy phenology in monsoon Asia using a continuous in situ dataset. Int. J. Remote Sens. 30, 4343–4357.

NSC, 2008. National Statistics Center of the Lao PDR Web Page: http://www.nsc.gov.la/ (accessed July 2008).

NSOP, 2008. National Statistics Office of Philippines Web Page: http://www.census.gov.ph/data/sectordata/dataagri.html (accessed July 2008).

NSOT, 2008. National Statistical Office of Thailand Web Page: http://web.nso.go.th/eng/index.htm (accessed July 2008).

Payne, V.H., Clough, S.A., Shephard, M.W., Nassar, R., Logan, J.A., 2009. Information-centered representation of retrievals with limited degrees of freedom for signal: application to methane from the tropospheric emission spectrometer. J. Geophys. Res. 114, D10307.

Peng, D., Huete, A.R., Huang, J., Wang, F., Sun, H., 2011. Detection and estimation of mixed paddy rice cropping patterns with MODIS data. Int. J. Appl. Earth Obs. 13, 13–23.

Pingali, P.L., Xuan, V.T., 1992. Vietnam: decollectivization and rice productivity growth. Econ. Devel. Cult. Change 40, 697–718.

Roy, D.P., Borak, J.S., Devadiga, S., Wolfe, R.E., Zheng, M., Descloitres, J., 2002. The MODIS land product quality assessment approach. Remote Sens. Environ. 83, 62–76.

Sakamoto, T., Van Phung, C., Kotera, A., Nguyen, K.D., Yokozawa, M., 2009. Analysis of rapid expansion of inland aquaculture and triple rice-cropping areas in a coastal area of the Vietnamese Mekong Delta using MODIS time-series imagery. Landscape Urban Plann 92, 34–46.

Sakamoto, T., Yokozawa, M., Toritani, H., Shibayama, M., Ishitsuka, N., Ohno, H., 2005. A crop phenology detection method using time-series MODIS data. Remote Sens. Environ. 96, 366–374.

Sun, H., Huang, J., Huete, A.R., Peng, D., Zhang, F., 2009. Mapping paddy rice with multi-date Moderate-Resolution Imaging Spectroradiometer (MODIS) data in China. J. Zhejiang Univ. Sci. A 10, 1509–1522.

Tingting, L., Chuang, L., 2010. Study on extraction of crop information using time-series MODIS data in the Chao Phraya Basin of Thailand. Adv. Space Res. 45, 775–784.

Wardlow, B.D., Egbert, S.L., 2008. Large-area crop mapping using time-series MODIS 250 m NDVI data: an assessment for the US central Great Plains. Remote Sens. Environ. 112, 1096–1116.

Wassmann, R., Neue, H.U., Lantin, R.S., Makarim, K., Chareonsilp, N., Buendia, L.V., Rennenberg, H., 2000. Characterization of methane emissions from rice fields

in Asia. II. Differences among irrigated, rainfed, and deepwater rice. Nutr. Cycl. Agroecosys. 58, 13–22.
Xiao, X., Boles, S., Liu, J., Zhuang, D., Frolking, S., Li, C., Salas, W., Moore III, B., 2005. Mapping paddy rice agriculture in southern China using multi-temporal MODIS images. Remote Sens. Environ. 95, 480–492.
Xiao, X., Boles, S., Frolking, S., Li, C., Babu, J.Y., Salas, W., Moore III, B., 2006. Mapping paddy rice agriculture in South and Southeast Asia using multi-temporal MODIS images. Remote Sens. Environ. 100, 95–113.
Xiong, X., Barnet, C., Maddy, E., Sweeney, C., Liu, X., Zhou, L., Goldberg, M., 2008. Characterization and validation of methane products from the atmospheric infrared sounder (AIRS). J. Geophys. Res. 113, G00A01.
Yan, X., Ohara, T., Akimoto, H., 2003. Development of region specific emission factors and estimation of methane emission from rice fields in the East, Southeast and South Asian countries. Glob. Change Biol. 9, 237–254.
Zha, Y., Gao, J., Ni, S., 2003. Use of normalized difference built-up index in automatically mapping urban areas from TM imagery. Int. J. Remote Sens. 24, 583–594.